Inorg. Chem. **2007**, *46*, 11405–11415

Thermally Induced Spin Transitions in Nitroxide–Copper(II)–Nitroxide Spin Triads Studied by EPR

Matvey Fedin,*,† Sergey Veber,†,‡ Igor Gromov,§ Ksenia Maryunina,† Sergey Fokin,† Galina Romanenko,† Renad Sagdeev,† Victor Ovcharenko,† and Elena Bagryanskaya*,†

International Tomography Center SB RAS, Novosibirsk 630090, Russia, Physical Chemistry Laboratory, Department of Chemistry and Applied Biosciences, ETH Zürich, 8093 Zürich, Switzerland, Novosibirsk State University, Novosibirsk 630090, Russia

Received July 20, 2007

Thermally induced spin transitions in a family of heterospin polymer chain complexes of Cu^{2+} hexafluoroacetylacetonate with two pyrazole-substituted nitronyl nitroxides are studied using electron paramagnetic resonance (EPR) spectroscopy. The structural rearrangements at low temperatures induce spin transitions in exchange-coupled spin triads of nitroxide–copper(II)–nitroxide. The values of exchange interactions in spin triads of studied systems are typically on the order of tens to hundreds of inverse centimeters. The large magnitude of exchange interaction determines the specific and very informative peculiarities in EPR spectra due to the predominant population of the ground state of a spin triad and spin exchange processes. The variety of these manifestations depending on structure and magnetic properties of spin triads are described. EPR is demonstrated as an efficient tool for the characterization of spin transitions and for obtaining information on the temperature-dependent sign and value of the exchange interaction in strongly coupled spin triads.

I. Introduction

The exchange-coupled complexes of transition ions and stable organic radicals have accumulated significant interest in the field of molecular magnetism over the past few decades,[1−7] and the electron paramagnetic resonance (EPR) has proven to be a powerful technique for studying the exchange interactions in these systems.[8−14] A new family of heterospin polymer-chain complexes of Cu^{2+} hexafluoroacetylacetonate ($Cu(hfac)_2$) with stable pyrazole-substituted nitronyl nitroxides (L^R) has been found recently (Scheme 1).[15−18] Two different motifs of the polymer chains can be obtained: a head-to-tail motif leading to the formation of subsequent two-spin copper(II)-nitroxide clusters, and a head-

* To whom correspondence should be addressed. E-mail: mfedin@tomo.nsc.ru (M.F.), elena@tomo.nsc.ru (E.B).
† International Tomography Center SB RAS.
‡ Novosibirsk State University.
§ ETH Zürich.

(1) Kahn, O. *Molecular Magnetism*; VCH Publishers: New York, 1993.
(2) *Molecular Magnetism: From Molecular Assemblies to the Devices*; Coronado, E., Delhae's, P., Gatteschi, D., Miller, J. S., Eds.; Nato ASI Series E; Applied Sciences, Kluwer Academic Publisher: Dordrecht, The Netherlands, 1996; Vol. 321.
(3) *Molecular Magnetism*; Itoh, K., Kinoshita, M., Eds.; Gordon and Breach Science Publisher: Amsterdam, The Netherlands, 2000.
(4) *Magnetism: Molecules to Materials I: Models and Experiments and Magnetism: Molecules to Material II: Molecule-Based Materials and Experiments*; Miller, J. S., Drillon, M., Eds.; Wiley-VCH: New York, 2001.
(5) *Molecular Magnets: Recent Highlights*; Linert, W., Verdaguer, M., Eds.; Springer-Verlag: Wien, Austria, 2003.
(6) Caneschi, A.; Gatteschi, D.; Rey. P. *Prog. Inorg. Chem.* **1991**, *39*, 331−429.
(7) Ovcharenko, V. I.; Sagdeev, R. Z. *Russ. Chem. Rev.* **1999**, *68*, 345−363.
(8) Bencini, A.; Gatteschi D. *EPR of Exchange Coupled Systems*; Springer-Verlag: Berlin, Germany, 1990.
(9) Gatteschi, D.; Barra, A. L.; Caneschi, A.; Cornia, A.; Sessoli, R.; Sorace, L. *Coord. Chem. Rev.* **2006**, *250*, 1514−1529.
(10) McInnes, E. J. L. *Sruct. Bonding* **2006**, *122*, 69−102.
(11) Piligkos, S.; Bill, E.; Collison, D.; McInnes, E. J. L.; Timco, G. A.; Weihe, H.; Winpenny, R. E. P.; Neese, F. *J. Amer. Chem. Soc.* **2007**, *129*, 760−761.
(12) Yoon, J.; Mirica, L. M.; Stack, T. D. P.; Solomon, E. I. *J. Am. Chem. Soc.* **2004**, *126*, 12586−12595.
(13) Ziessel, R.; Stroh, C.; Heise, H.; Kohler, F. H.; Turek, P.; Claiser, N.; Souhassou, M.; Lecomte, C. *J. Am. Chem. Soc.* **2004**, *126*, 12604−12613.
(14) Maekawa, K.; Shiomi, D.; Ise, T.; Sato, K.; Takui, T. *J. Phys. Chem. B.* **2005**, *109*, 3303−3309.
(15) Ovcharenko, V. I.; Fokin, S. V.; Romanenko, G. V.; Shvedenkov, Yu. G.; Ikorskii, V. N.; Tretyakov, E. V.; Vasilevskii, S. F. *J. Struct. Chem.* **2002**, *43*, 153−167.
(16) Rey, P.; Ovcharenko, V. I. Copper(II) Nitroxide Molecule Spin-Transition Complexes. In *Magnetism: Molecules to Materials IV*; Miller, J. S., Drillon, M., Eds.; Wiley-VCH: New York, 2003; pp 41−63.
(17) Ovcharenko, V. I.; Fokin, S. V.; Romanenko, G. V.; Ikorskii, V. N.; Tretyakov, E. V.; Vasilevskii, S. F.; Sagdeev, R. Z. *Mol. Phys.* **2002**, *100*, 1107−1115.
(18) Ovcharenko, V. I.; Maryunina, K. Yu.; Fokin, S. V.; Tretyakov, E. V.; Romanenko, G. V.; Ikorskii, V. N. *Russ. Chem. Bull., Int. Ed.* **2004**, *53*, 2406−2427.

10.1021/ic7014385 CCC: $37.00
Published on Web 11/21/2007

Scheme 1. (a) Chemical Structure of $Cu(hfac)_2$ and the Nitroxide Ligand L^R and (b) Typical Polymer-Chain Structure of $Cu(hfac)_2L^R$ Complexes ($Cu(hfac)_2L^{Pr}$ is Shown)

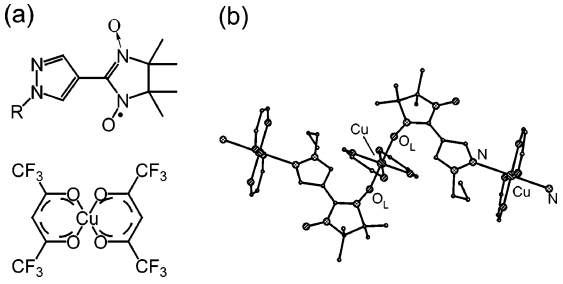

to-head motif leading to a formation of an alternating one-spin copper(II) and three-spin nitroxide−copper(II)−nitroxide clusters. It was found that these complexes undergo reversible structural rearrangements at low temperatures, where the Cu−O bond lengths may change by up to 0.3 Å. The latter leads to pronounced changes in the value and possibly in the sign of the exchange interaction in spin triads and induces the magnetic anomalies in the temperature dependences of the effective magnetic moment $\mu_{eff}(T)$ similar to a classical spin crossover. The predominant population of a particular spin state of the whole exchange-coupled cluster may occur during such a spin transition, and the character of transition does depend strongly on the substituent R of the nitroxide ligand. Note, that similar magnetic anomalies have also been observed for other complexes of copper(II) with nitroxides previously[19−22] and in a recent work.[23]

The thermally induced structural changes and conjugated with them spin transitions in the family $Cu(hfac)_2L^R$ have been investigated previously using the X-ray and magnetic susceptibility techniques.[15,17,18] Recently, the first EPR study of the propyl-substituted compound $Cu(hfac)_2L^{Pr}$ has been reported.[24] The polymer chains of $Cu(hfac)_2L^{Pr}$ have a head-to-head motif, and all of the magnetic anomalies are due to the rearrangements occurring in the three-spin units >N−•O−Cu^{2+}−O•−N<. Very unusual temperature-dependent EPR spectra were registered experimentally and explained theoretically. The strong antiferromagnetic exchange in a spin triad leads to a predominant population of the lowest spin state $S = {}^1/_2$, which has a g factor smaller than two. This occurs at relatively high temperatures $T < 140$ K and, as a result, the EPR spectrum displays the unusual signals with $g < 2$, which are very strong and highly informative. In particular, the appearance of $g < 2$ signals unambiguously indicates that the exchange interaction is antiferromagnetic (negative) and comparable to or higher than thermal energy kT. Further investigations have shown that the position of these $g < 2$ signals is temperature dependent at $kT \sim |J|$ because of the electron spin exchange process between different multiplets of a spin triad.[25] It was also proposed that the value of the exchange interaction and its temperature dependence can be obtained by monitoring the shift of the $g < 2$ signal.

In the present work, we report the EPR study of compounds $Cu(hfac)_2L^R$ with various alkyl substituents R = ethyl (Et), propyl (Pr), butyl (Bu), and $Cu(hfac)_2L^{Bu}$•0.5Solv with various organic solvents (Solv) included into a crystal structure. We describe the rules for understanding the spectra, obtaining the sign, and estimating the value of the exchange interaction in strongly coupled spin triads as well as the character of its change during spin transitions.

II. Experimental Section

Synthesis of the Compounds. 4,4,5,5-Tetramethyl-2-(1-R-1*H*-pyrazol-4-yl)-imidazoline-3-oxide-1-oxyl (L^R), $Cu(hfac)_2L^R$ (R = Et, Pr), and $Cu(hfac)_2L^{Bu}$•$0.5C_6H_{14}$ were synthesized according to a known procedure.[15−18] All of the other compounds $Cu(hfac)_2L^{Bu}$•0.5Solv were synthesized in the same manner as $Cu(hfac)_2L^{Bu}$•$0.5C_6H_{14}$.[17]

$Cu(hfac)_2L^{Bu}$•$0.5C_7H_{16}$. A mixture of $Cu(hfac)_2$ (0.089 g, 0.19 mmol) and L^{Bu} (0.052 g, 0.19 mmol) was dissolved with heating up to 75 °C in heptane (15 mL). The resulting dark-brown solution was allowed to slowly evaporate in an open flask at 5 °C. After 1 day, large dark-violet rhombohedral crystals were formed; they were filtered off, quickly washed with cold heptane, and dried in air. Yield: 0.109 g, 71%. Anal. Calcd for $C_{27.5}H_{33}N_4O_6F_{12}Cu$: C, 40.9; H, 4.1; N, 6.9; F, 28.3. Found: C, 40.6; H, 4.5; N, 6.8; F, 27.9.

$Cu(hfac)_2L^{Bu}$•$0.5C_8H_{18}$. A mixture of $Cu(hfac)_2$ (0.048 g, 0.10 mmol) and L^{Bu} (0.028 g, 0.10 mmol) was dissolved in acetone (0.5 mL) and then octane (5 mL) was added. The resulting dark-brown solution was allowed to slowly evaporate in an open flask at 5 °C. After 2 days, large dark-violet rhombohedral crystals were formed; they were filtered off, quickly washed with cold heptane, and dried in air. Yield: 0.060 g, 71%. Anal. Calcd for $C_{28}H_{34}N_4O_6F_{12}Cu$: C, 41.3; H, 4.2; N, 6.9; F, 28.0. Found: C, 41.0; H, 4.1; N, 6.6; F, 27.9.

$Cu(hfac)_2L^{Bu}$•$0.5C_8H_{16}$. A mixture of $Cu(hfac)_2$ (0.096 g, 0.20 mmol) and L^{Bu} (0.056 g, 0.20 mmol) was dissolved with heating up to 75 °C in octene (1.5 mL). The resulting dark-brown solution was allowed to slowly evaporate in an open flask at 5 °C. After 3−4 h, dark-violet rhombohedral crystals were formed; they were filtered off, quickly washed with cold heptane, and dried in air. Yield: 0.063 g, 78%. Anal. Calcd for $C_{28}H_{33}N_4O_6F_{12}Cu$: C, 41.4; H, 4.1; N, 6.9; F, 28.0. Found: C, 41.2; H, 4.1; N, 6.7; F, 27.8.

$Cu(hfac)_2L^{Bu}$. A mixture of $Cu(hfac)_2$ (0.048 g, 0.10 mmol) and L^{Bu} (0.028 g, 0.10 mmol) was dissolved in acetone (1 mL) and then decane (3 mL) was added. The resulting dark-brown solution was slowly concentrated with a flow of air to a volume of 3 mL. After 6−8 h, dark-violet elongated crystals were formed; they were filtered off, quickly washed with cold heptane, and dried in air. Yield: 0.041 g, 54%. Anal. Calcd for $C_{24}H_{25}N_4O_6F_{12}Cu$: C, 38.1; H, 3.3; N, 7.4; F, 30.1. Found: C, 38.1; H, 3.6; N, 7.2; F, 29.9.

$Cu(hfac)_2L^{Bu}$•$0.5C_6H_6$. A mixture of $Cu(hfac)_2$ (0.048 g, 0.10 mmol) and L^{Bu} (0.028 g, 0.10 mmol) was dissolved in benzene (1 mL). The resulting dark-brown solution was allowed to slowly

(19) Caneschi, A.; Chiesi, P.; David, L.; Ferraro, F.; Gatteschi, D.; Sessoli, R. *Inorg. Chem.* **1993**, *32*, 1445−1453.
(20) Lanfranc de Panthou, F.; Belorizky, E.; Calemczuk, R.; Luneau, D.; Marcenat, C.; Ressouche, E.; Turek, P.; Rey, P. *J. Am. Chem. Soc.* **1995**, *117*, 11247−11253.
(21) Lanfranc de Panthou, F.; Luneau, D.; Musin, R.; Ohrstrom, L.; Grand, A.; Turek, P.; Rey, P. *Inorg. Chem.* **1996**, *35*, 3484−3491.
(22) Iwahory, F.; Inoue, K.; Iwamura, H. *Mol. Cryst. Liq. Cryst.* **1999**, *334*, 533−538.
(23) Baskett, M.; Lahti, P. M.; Paduan-Filho, A.; Oliveira, N. F. *Inorg. Chem.* **2005**, *44*, 6725−6735.
(24) Fedin, M.; Veber, S.; Gromov, I.; Ovcharenko, V.; Sagdeev, R.; Schweiger, A.; Bagryanskaya, E. *J. Phys. Chem. A* **2006**, *110*, 2315−2317.
(25) Fedin, M.; Veber, S.; Gromov, I.; Ovcharenko, V.; Sagdeev, R.; Bagryanskaya, E. *J. Phys. Chem. A* **2007**, *111*, 4449−4455.

evaporate in an open flask at 5 °C. After 2 days, dark-violet rhombohedral crystals were formed; they were filtered off, quickly washed with cold heptane, and dried in air. Yield: 0.057 g, 71%. Anal. Calcd for $C_{27}H_{28}N_4O_6F_{12}Cu$: C, 40.7; H, 3.5; N, 7.0; F, 28.6. Found: C, 41.0; H, 3.9; N, 6.9; F, 28.7. **Cu(hfac)$_2$L^{Bu}·0.5C$_7$H$_8$** and **Cu(hfac)$_2$L^{Bu}·0.5C$_8$H$_{10}$** were prepared by a similar procedure using appropriate solvents. **Cu(hfac)$_2$L^{Bu}·0.5C$_7$H$_8$.** Yield: 0.035 g, 44%. Anal. Calcd for $C_{27.5}H_{29}N_4O_6F_{12}Cu$: C, 41.1; H, 3.6; N, 7.0; F, 28.4. Found: C, 41.7; H, 4.0; N, 6.9; F, 28.5. **Cu(hfac)$_2$L^{Bu}·0.5C$_8$H$_{10}$.** Yield: 0.058 g, 71%. Anal. Calcd for $C_{28}H_{30}N_4O_6F_{12}$-Cu: C, 41.5; H, 3.7; N, 6.9; F, 28.1. Found: C, 41.2; H, 3.5; N, 6.9; F, 28.2.

All complexes **Cu(hfac)$_2$L^{Bu}·0.5Solv** (Solv = C_7H_{16}, C_8H_{18}, C_8H_{16}, C_6H_6, C_7H_8, and C_8H_{10}) and **Cu(hfac)$_2$L^{Bu}** are soluble in most organic solvents. When stored in solution at room temperature for 2 days or more, they gradually decompose. When stored in air, crystals Cu(hfac)$_2$L^{Bu}·0.5Solv gradually lose solvent molecules and become turbid. This process develops especially quickly for solids **Cu(hfac)$_2$L^{Bu}·0.5C$_8$H$_{16}$** and **Cu(hfac)$_2$L^{Bu}·0.5C$_8$H$_{18}$**, which lose their solvents completely during 2 days at room temperature.

EPR Measurements. The experiments have been carried using a commercial X-band (9 GHz) EPR spectrometer (Bruker Biospin Elexsys E580), a commercial W-band (94 GHz) EPR spectrometer (Bruker Biospin Elexsys E680), and a home-built Q-band (35 GHz) EPR spectrometer[26] in continuous wave mode. In all of the experiments reported in this work, the polycrystalline powders of the compounds Cu(hfac)$_2$L^R were used. To obtain the powder pattern, EPR spectra at several sample orientations have usually been recorded and summed up. In addition, when necessary the polycrystalline powder has been preliminarily crushed. The severe crushing produced defects in the polymer-chain structure, leading to an appearance of signals from free nitroxides (g = 2.007). Because this was undesired, an optimum between the strength of the nitroxides' signals and the quality of the EPR powder pattern has been adjusted. For the W-band study, where the sample volume is small, this complication often resulted in the unavoidable presence of these additional signals in the EPR spectra. To get rid of the effect of the microcrystals' alignment along the strong magnetic field at the W band, the polycrystalline powder Cu(hfac)$_2$L^R was preliminary mixed with a well-crushed diamagnetic quartz powder. The alignment effects at the X and Q bands have been found insignificant.

X-ray Structure. The data were collected on a Smart Apex with a CCD detector (BRUKER AXS, Germany) automatic diffractometer using Mo Kα radiation. The structures were solved by direct methods and refined anisotropically by a full-matrix least-squares analysis. The hydrogen atoms were partially localized on difference electron-density maps and refined isotropically together with non-hydrogen atoms. All of the calculations and refinements were carried out using *SXTL* software. A part of the structural data on Cu(hfac)$_2$L^{Et} and Cu(hfac)$_2$L^{Pr} was published earlier[15] and has been included in Cambridge Structural Data Base (CSDB) (Cu(hfac)$_2$L^{Et}, T = 115, 188, and 295 K, REFCODEs LUPNOZ, LUPNOZ01, and LUPNOZ02; Cu(hfac)$_2$L^{Pr}, T = 115, 203, and 295 K, REFCODEs LUPPIV, LUPPIV01, and LUPPIV02).

Magnetic Measurements. Measurements were carried out on a Quantum Design SQUID magnetometer MPMS-5S in the temperature range 2−300 K (magnetic field strength 0.5 T). The paramagnetic susceptibility (χ) was calculated by taking into account the diamagnetic contributions of atoms according to Pascal's scheme. The effective magnetic moment was calculated by the formula $\mu_{eff} = [(3k/N\beta^2)\chi T]^{1/2} \approx (8\chi T)^{1/2}$, where k is the Boltzmann's constant, N is Avogadro's number, and β is the Bohr magneton.

(26) Gromov, I.; Shane, J.; Forrer, J.; Rakhmatoullin, R.; Rosenzwaig, Y.; Schweiger, A. *J. Magn. Reson.* **2001**, *149*, 196−203.

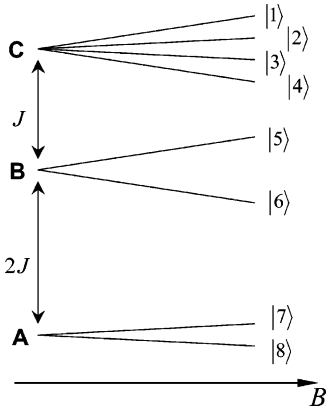

Figure 1. Energy levels scheme of an exchange-coupled spin triad with $|J| \gg B$, $J < 0$.

III. Results and Discussion

Theoretical Background. The spin-Hamiltonian of the symmetric exchange-coupled spin-triad nitroxide−copper(II)−nitroxide can be written in the following form

$$\hat{H} = \beta \boldsymbol{B}\boldsymbol{g}^{R}(\boldsymbol{S}^{R1} + \boldsymbol{S}^{R2}) + \beta \boldsymbol{B}\boldsymbol{g}^{Cu}\boldsymbol{S}^{Cu} - 2J(\boldsymbol{S}^{R1} + \boldsymbol{S}^{R2})\boldsymbol{S}^{Cu} - 2J'\boldsymbol{S}^{R1}\boldsymbol{S}^{R2} \quad (1)$$

where the superscripts R1 and R2 correspond to the two nitroxides and Cu to the copper, and $\boldsymbol{g}^{R}$ and $\boldsymbol{g}^{Cu}$ are the corresponding g tensors. The nitroxides are assumed to be equivalent with an isotropic g factor g^R, that is, $\boldsymbol{g}^{R} = g^{R}\hat{\mathbf{1}}$, where $\hat{\mathbf{1}}$ is the unity matrix. $\boldsymbol{B} = [0,0,B]$ is the magnetic field along the z axis, J corresponds to the exchange interaction between copper and each nitroxide, and J' to the exchange interaction between nitroxides ($J < 0$ corresponds to the antiferromagnetic coupling). For the linear geometry of a spin triad, J' is considerably smaller than J, and therefore the last term in eq 1 can safely be neglected for our cases.

The energy level scheme of a spin triad for the case $|J| \gg B$ and $J < 0$ is shown in Figure 1. In all of the spin triads studied in this work, the exchange interaction is antiferromagnetic, therefore we will always consider this case in the following discussion. The corresponding eigenfunctions for $B = 0$ in the basis $|S_z^{R1}\, S_z^{Cu}\, S_z^{R2}\rangle$ ($\alpha = +1/2$, $\beta = -1/2$) can be found as[25]

$$|1\rangle = |\alpha\alpha\alpha\rangle$$
$$|2\rangle = \{(|\alpha\alpha\beta\rangle + |\beta\alpha\alpha\rangle + |\alpha\beta\alpha\rangle)\}/\{\sqrt{3}\}$$
$$|3\rangle = \{(|\alpha\beta\beta\rangle + |\beta\beta\alpha\rangle + |\beta\alpha\beta\rangle)\}/\{\sqrt{3}\}$$
$$|4\rangle = |\beta\beta\beta\rangle$$
$$|5\rangle = \{(|\alpha\alpha\beta\rangle - |\beta\alpha\alpha\rangle)\}/\{\sqrt{2}\}$$
$$|6\rangle = \{(|\alpha\beta\beta\rangle - |\beta\beta\alpha\rangle)\}/\{\sqrt{2}\}$$
$$|7\rangle = \{(|\alpha\alpha\beta\rangle + |\beta\alpha\alpha\rangle - 2|\alpha\beta\alpha\rangle)\}/\{\sqrt{6}\}$$
$$|8\rangle = \{(|\alpha\beta\beta\rangle + |\beta\beta\alpha\rangle - 2|\beta\alpha\beta\rangle)\}/\{\sqrt{6}\} \quad (2)$$

The energy values of the three multiplets A ($S = {}^1/_2$), B ($S = {}^1/_2$), and C ($S = {}^3/_2$) are $E^A = 2J$, $E^B = 0$, and $E^C = -J$, and corresponding effective g tensors can be found as[27]

$$\boldsymbol{g}^A = \{(4g^R\hat{\mathbf{1}} - \boldsymbol{g}^{Cu})\}/\{3\}$$
$$\boldsymbol{g}^B = \boldsymbol{g}^{Cu}$$
$$\boldsymbol{g}^C = \{(2g^R\hat{\mathbf{1}} + \boldsymbol{g}^{Cu})\}/\{3\} \quad (3)$$

The phenomenological description of spin transitions occurring in spin triads of compounds $Cu(hfac)_2L^R$ is straightforward. At high temperatures where the thermal energy kT exceeds the value of the exchange interaction ($kT \gg |J|$), all of the spin states $S = {}^1/_2$ and $S = {}^3/_2$ are nearly equally populated, and the Boltzman factor $|J|/kT$ is small (Figure 1). Structural rearrangements in octahedral units CuO_6 at lower temperatures lead to the significant shortening or lengthening of the Cu−O distances[15,16] and, consequently, to the changes of the exchange-interaction magnitude. The former is exemplified in Figure 2, where the temperature dependences of the Cu−O_L (CuO_6 unit) and Cu−N_L (CuO_4N_2 unit) distances in $Cu(hfac)_2L^{Pr}$ are shown. As a result, the factor $|J|/kT$ may change significantly. For most of the compounds $Cu(hfac)_2L^R$, this occurs because of the simultaneous increase of $|J|$ and decrease of T, resulting in the predominant population of the ground state A ($S = {}^1/_2$).

The effective magnetic moment of a spin triad can be calculated as

$$\mu_{eff}{}^2(T) = \sum_{I = A,B,C} (g^I)^2 S^I(S^I + 1)K_B^I \quad (4)$$

where g^I and S^I are the average (isotropic) g value and the total spin of the multiplets A, B, and C. The factors K_B^I take account of the Boltzman populations of the corresponding multiplets

$$K_B^I = \frac{(2S^I + 1) \cdot e^{-E^I/kT}}{\sum_{P = A,B,C} (2S^P + 1)e^{-E^P/kT}} \quad (5)$$

E^I are the energies of the corresponding multiplets, where for the case $B \ll |J|$ we can safely neglect Zeeman energy differences between $(2S + 1)$ states of each multiplet. Then, for the antiferromagnetic exchange ($J < 0$) the temperature dependence of the effective magnetic moment of a spin triad can be written using eqs 4 and 5 as

$$\mu_{tr,eff}{}^2(T) = \frac{3(g^A)^2 + 3(g^B)^2 \cdot e^{2J/kT} + 30(g^C)^2 \cdot e^{3J/kT}}{4(1 + e^{2J/kT} + 2e^{3J/kT})} \quad (6)$$

When $|J|/kT \approx 0$, one obtains $\mu_{tr,eff}{}^2 = [3(g^A)^2 + 3(g^B)^2 + 30(g^C)^2]/16$, which gives $\mu_{tr,eff} = 3\beta$ for $g^A = g^B = g^C = 2$ and corresponds to three uncoupled electron spins $S = {}^1/_2$. When $|J|/kT \gg 1$, $J < 0$ one obtains $\mu_{tr,eff}{}^2 = 3(g^A)^2/4$, which for $g^A = 2$ gives $\mu_{tr,eff} = \sqrt{3} \approx 1.73\ \beta$, corresponding to one spin $S = {}^1/_2$. Therefore, the noticeable change in magnetic moment should occur by passing from the situation $|J|/kT \approx 0$ to the situation $|J|/kT \gg 1$.

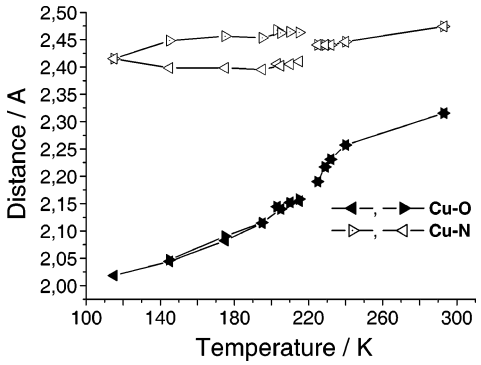

Figure 2. Temperature dependences of the Cu−O_L (CuO_6 unit) and Cu−N_L (CuO_4N_2 unit) distances in $Cu(hfac)_2L^{Pr}$ obtained by X-ray study (O_L and N_L atoms belong to the nitroxide groups). Two sets of each data at $T < 226$ K reflect the lowering of the symmetry of the unit cells below the phase transition (space group $C2/c$ at $T > 226$ K, and $P2_1/c$ at $T < 226$ K).[15,18]

If the exchange interaction itself is a function of temperature $J = J(T)$, which is the case for the compounds $Cu(hfac)_2L^R$, the factor $|J|/kT$ may change significantly within a narrow temperature range, especially if J changes abruptly during structural rearrangements. An additional factor influencing the amplitude of change of $\mu_{tr,eff}$ is the significant difference in effective g values of multiplets A, B, and C for spin triads of nitroxide−copper(II)−nitroxide. Reasonable values $g^{Cu} \approx 2.15$ (isotropic value) and $g^R \approx 2.007$ lead to $g^A = 1.96$, $g^B = 2.15$, and $g^C = 2.05$, and thus we arrive at $\mu_{tr,eff} = 3.077\ \beta$ for $|J|/kT \approx 0$ and $\mu_{tr,eff} = 1.697\ \beta$ for $|J|/kT \gg 1$, $J < 0$.

As was mentioned above, the polymer chains of the compounds $Cu(hfac)_2L^R$ may have a head-to-tail or head-to-head motif depending on how the copper ion is coordinated by nitroxides. In this work, we focus on compounds having a head-to-head motif of the polymer chains, which contain the alternating one-spin copper(II) and three-spin nitroxide−copper(II)−nitroxide systems. Because of the presence of these two types of paramagnetic centers, both EPR and magnetic susceptibility data are described as the superposition of two contributions. In magnetic susceptibility measurements, an integral susceptibility is obtained, and then an effective magnetic moment corresponding to the single copper center is calculated. Thus, the experimentally measured value is

$$\mu_{eff}{}^2 = 0.5\mu_{tr,eff}{}^2 + 0.5\mu_{is,eff}{}^2 = \frac{3(g^A)^2 + 3(g^B)^2 \cdot e^{2J/kT} + 30(g^C)^2 \cdot e^{3J/kT}}{8(1 + e^{2J/kT} + 2e^{3J/kT})} + 0.5\mu_{is,eff}{}^2 \quad (7)$$

where subscripts "tr" and "is" correspond to the spin triad and the isolated copper ion, respectively. In many situations considered below, the exchange interaction between a triad and an isolated copper is significantly smaller than the exchange interaction within a spin triad. The exchange interaction between a triad and an isolated copper (inter-

(27) Benelli, C.; Gatteschi, D.; Zanchini, C.; Latour, J. M.; Rey, P. *Inorg. Chem.* **1986**, *25*, 4242−4244.

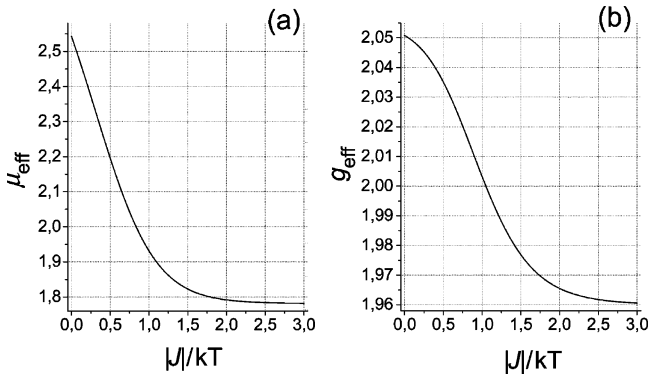

Figure 3. (a) Dependence μ_{eff} versus $|J|/kT$ ($J < 0$) calculated for Cu(hfac)$_2$L^R using eq 7 and assuming $\mu_{is,eff} \approx 1.86\,\beta$. (b) The dependence g_{eff} versus $|J|/kT$ ($J < 0$) calculated for Cu(hfac)$_2$L^R using eq 10. Typical average g values $g^A = 1.96$, $g^B = 2.15$, and $g^C = 2.05$ are used.

cluster exchange) significantly influences the magnetic susceptibility curves at low temperatures (typically <20 K) only. Thus, for simple estimations one can neglect this intercluster exchange interaction at higher temperatures and use the temperature-independent value $\mu_{is,eff} \approx 1.86\,\beta$, which corresponds to the uncoupled spin $S = {}^1/_2$ of copper with an average $g \approx 2.15$. Part a of figure 3 shows the calculated dependence of μ_{eff} versus $|J|/kT$ for this case.

The eqs 4−7 are capable of phenomenologically describing the so-called nonclassical spin transitions in the strongly coupled spin triads of nitroxide−copper(II)−nitroxide.[15,17,18] The arbitrary function $J(T)$ may be used, which makes the description of various dependencies $\mu_{eff}(T)$ possible. Generally, one cannot obtain the function $J(T)$ by fitting the experimental dependence $\mu_{eff}(T)$ without the knowledge of corresponding g tensors, therefore the EPR measurements are topical. The present work is not aimed at obtaining the functions $J(T)$ for the studied compounds; however, we will use eq 7 and part a of Figure 3 below for qualitative correlations of the EPR and magnetic susceptibility data.

EPR of Strongly Coupled Spin Triads. Similarly to the discussion in the previous section, the description of nonclassical spin transitions in EPR requires the consideration of temperature-dependent Boltzman populations of different multiplets of a spin triad and an account of the dependence of the exchange interaction on temperature $J(T)$.

We have found recently[24,25] that spin triads coupled by a strong exchange interaction $|J| > kT$ manifest specific characteristics in EPR due to the predominant population of the ground state of a spin triad and the electron spin-exchange process between different multiplets. These two effects determine the line shapes and positions in the EPR spectra and their temperature-dependent evolution.

At relatively high temperatures $kT \gg |J|$, the EPR spectrum of a spin triad should consist of three groups of lines described by g tensors $\boldsymbol{g}^A$, $\boldsymbol{g}^B$, and $\boldsymbol{g}^C$. However, at low temperatures $kT \ll |J|$ ($J < 0$) the populations of multiplets B and C are negligible, and basically only the ground multiplet A is populated. As a result, the EPR signals with $\boldsymbol{g}^B$ and $\boldsymbol{g}^C$ are not observed, whereas the signals with $\boldsymbol{g}^A$ are strongly enhanced, what we referred to as a static multiplet polarization of a spin triad.[24] The signals with $\boldsymbol{g}^A < 2$ are well separated from the rest of the spectrum and therefore are useful in many respects. As we have mentioned above, in all of the spin triads studied in this work the exchange interaction is antiferromagnetic. However, for the case of the strong ferromagnetic exchange interaction ($J > 0$) one would expect different behavior at low temperatures: the enhancement of signals with $\boldsymbol{g}^C$ and the virtual absence of signals with $\boldsymbol{g}^A$ and $\boldsymbol{g}^B$. Thus, the EPR spectra of spin triads at temperatures $kT < |J|$ are indicative of the sign of the exchange interaction.[24]

At higher temperatures $kT \sim |J|$ and $kT > |J|$, one would expect that the relative intensities of the signals with $\boldsymbol{g}^A$, $\boldsymbol{g}^B$, and $\boldsymbol{g}^C$ will change, reflecting the Boltzman population change of multiplets A, B, and C. However, the experimentally observed temperature evolution of the EPR spectra is more complicated. In most of the cases, we observed a single broad line at $kT > |J|$, whose position, that is, effective g factor $\boldsymbol{g}_{eff}$, is temperature dependent. At $kT \ll |J|$, $\boldsymbol{g}_{eff}$ corresponds to $\boldsymbol{g}^A$, then $\boldsymbol{g}_{eff}$ increases with temperature, and at $kT \gg |J|$ it corresponds to $\boldsymbol{g}^C = (\boldsymbol{g}^A + \boldsymbol{g}^B)/2$. This peculiar behavior was explained by fast transitions between different multiplets, which we call the electron spin exchange process by analogy with a similar effect well-known for radicals in solution.[25] If the rate of spin exchange is high compared to the frequency differences between EPR lines, the single exchange-narrowed line with $\boldsymbol{g}_{eff}$ is observed in the center of mass of the spectrum. Because the contributions from EPR lines of multiplets B and C increase with increasing temperature, the center of mass shifts toward higher g values, which completely explains the experimentally observed temperature shift of the EPR line of the spin triad. We have proposed and supported by estimations that the mechanism causing the spin exchange in Cu(hfac)$_2$L^R is the modulation of the copper−nitroxide exchange interaction by lattice vibrations. For $|J| \sim 100$ cm^{-1}, the rate of the spin exchange can be up to $\sim 10^{12}$ s^{-1}, which implies the fast exchange conditions even at W-band EPR frequency (94 GHz).[25]

For the case of fast spin exchange, one obtains the equations for the center of the mass of the spectrum $g_{eff}(T)$ in a similar way to that for eqs 4−7

$$\boldsymbol{g}_{eff}(T) = \{\sum_{I=A,B,C} \boldsymbol{g}^I P_B^I\}/\{\sum_{I=A,B,C} P_B^I\} = \frac{\boldsymbol{g}^A P_B^A + \boldsymbol{g}^B P_B^B + \boldsymbol{g}^C P_B^C}{P_B{}^A + P_B{}^B + P_B{}^C} \quad (8)$$

where P_B^I describe the probabilities of the microwave absorption by an electron in states A, B, or C. The coefficients P_B^I take account of the Boltzman population factor, the number of EPR transitions within each multiplet, and the probabilities of the corresponding EPR transitions

$$P_B{}^I = e^{-E^I/kT} \sum_i p_i{}^I \quad (9)$$

where p_i^I is the intensity of EPR transitions within a multiplet I. One EPR transition $|7\rangle \leftrightarrow |8\rangle$ is allowed within multiplet A, one EPR transition $|5\rangle \leftrightarrow |6\rangle$ is allowed within multiplet B, and three EPR transitions $|1\rangle \leftrightarrow |2\rangle$, $|2\rangle \leftrightarrow |3\rangle$

and $|3\rangle \leftrightarrow |4\rangle$ are allowed within multiplet C. The corresponding transition intensities are proportional to $m_{ij}^2 = |\langle i|\hat{S}_x|j\rangle|^2$, which can be found to be $m_{12}^2 = m_{34}^2 = {}^3/_4$, $m_{23}^2 = 1$ and $m_{56}^2 = m_{78}^2 = {}^1/_4$. Using these relations and eqs 8 and 9, we finally arrive at

$$\boldsymbol{g}_{\mathbf{eff}}(T) = \frac{\boldsymbol{g}^{\mathrm{A}} + \boldsymbol{g}^{\mathrm{B}} \cdot e^{2J/kT} + 10\boldsymbol{g}^{\mathrm{C}} \cdot e^{3J/kT}}{1 + e^{2J/kT} + 10e^{3J/kT}} \qquad (10)$$

For the high-temperature limiting case $|J|/kT \approx 0$, one finds $\boldsymbol{g}_{\mathbf{eff}} = \boldsymbol{g}^{\mathrm{C}}$, because $\boldsymbol{g}^{\mathrm{A}} + \boldsymbol{g}^{\mathrm{B}} = 2\boldsymbol{g}^{\mathrm{C}}$ according to (3), whereas for the low-temperature case where $|J|/kT \gg 1$, $J < 0$, one obtains $\boldsymbol{g}_{\mathbf{eff}} = \boldsymbol{g}^{\mathrm{A}}$. This means that for reasonable average (isotropic) values $g^{\mathrm{A}} = 1.96$ and $g^{\mathrm{C}} = 2.05$ the effective g factor is expected to shift by nearly $\Delta g_{\mathrm{eff}} \sim 0.1$ with temperature. At W-band frequency 94 GHz, this corresponds to a ~150 mT shift of the resonance magnetic field, which can easily be monitored. Similar to the temperature dependence of the effective magnetic moment, the effective g value reflects the dependence $J(T)$ and may change jumplike or smoothly depending on this function. It is useful to note that, the relation $g_{\mathrm{eff}} \approx g^{\mathrm{R}} \approx 2$ holds for $|J| \approx kT$, $J < 0$, which can be derived from eqs 10 and 3 and is seen from part b of Figure 3. Thus, the temperature at which the EPR line of a spin triad crosses the value $g = 2$ can be used for the simple estimation of the exchange-interaction value (at this certain temperature). Another useful trait is that when the parameter $|J|/kT$ ($J < 0$) reaches the value ~2, the effective g factor g_{eff} almost reaches its minimum value g^{A}: about 90% of the transformation $g_{\mathrm{eff}} = g^{\mathrm{C}} \rightarrow g_{\mathrm{eff}} = g^{\mathrm{A}}$ is completed, which can also be used for the estimations of J. These two estimations are visualized in part b of Figure 3, which shows the dependence of g_{eff} on the parameter $|J|/kT$ calculated using eq 10 for the typical average (isotropic) g values $g^{\mathrm{A}} = 1.96$, $g^{\mathrm{B}} = 2.15$ and $g^{\mathrm{C}} = 2.05$. The shape of the curve of $g_{\mathrm{eff}}(|J|/kT)$ is somewhat different compared to that of $\mu_{\mathrm{eff}}(|J|/kT)$ calculated using eq 7 (part a of Figure 3), which also is an important point for the interpretation of experimental results.

Spin Transitions in Cu(hfac)$_2$L$^{\mathbf{R}}$. In this section, we describe the experimental manifestation of different spin transitions in EPR using the family of compounds Cu(hfac)$_2$L$^{\mathrm{R}}$. As was mentioned above, two types of paramagnetic centers (one- and three-spin systems) are contained in polymer chains of Cu(hfac)$_2$L$^{\mathrm{R}}$ (part b of Scheme 1). Therefore, we observe two types of signals, one corresponding to the isolated copper ion in the >N−Cu−N< unit (with g tensor $\boldsymbol{g}^{\mathbf{Cu}}_{\mathrm{isolated}}$) and another one corresponding to the spin triad in the >N−•O−Cu−O•−N< unit. These two types of signals are very well separated by their g values in many situations.[24,25] The positions of signals of isolated copper ion remain virtually temperature independent and correspond to $g > 2$. As an example clarifying the two contributions, the signals of the isolated copper ion and of a spin triad are marked on the top spectra of Figure 4.

The different character of temperature-dependent structural rearrangements in Cu(hfac)$_2$L$^{\mathrm{R}}$ results in different dependencies $J(T)$ and different manifestations of spin transitions.

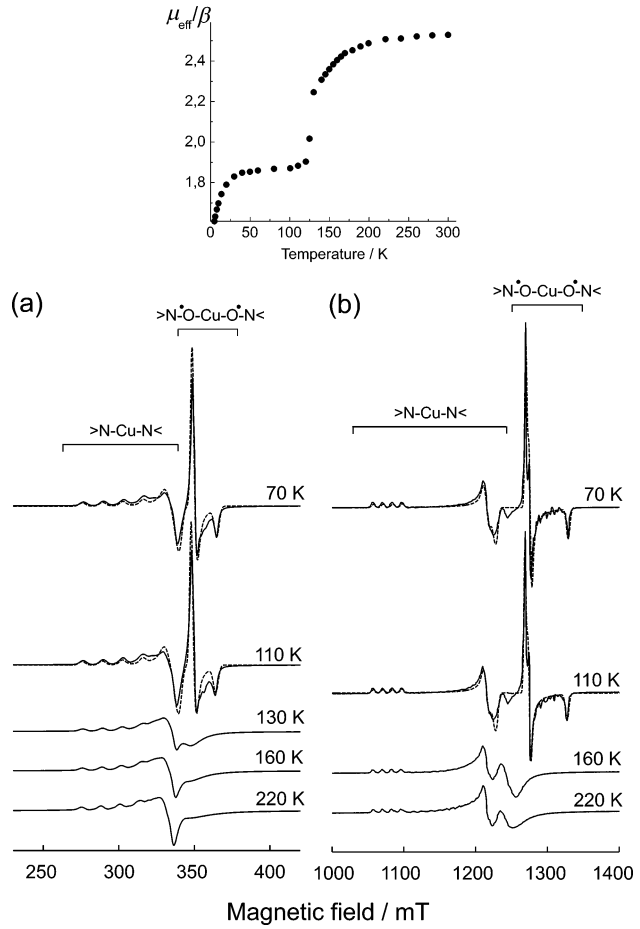

Figure 4. CW EPR spectra at different T (a,b) and dependence $\mu_{\mathrm{eff}}(T)$ (inset) of Cu(hfac)$_2$L$^{\mathrm{Bu}}$•0.5C$_7$H$_{16}$. (a) X band ($\nu_{\mathrm{mw}} \approx 9.714$ GHz, $B \approx 347$ mT at $g_{\mathrm{eff}} = 2$). (b) Q band ($\nu_{\mathrm{mw}} \approx 35.395$ GHz, $B \approx 1264$ mT at $g_{\mathrm{eff}} = 2$). The temperatures are indicated on the right; the curves are scaled. Calculation parameters for $T = 110$ K: $\boldsymbol{g}^{\mathbf{Cu}} = [2.048, 2.078, 2.314]$, $g^{\mathrm{R}} = 2.007$, $J = -200$ cm^{-1}; $\boldsymbol{g}^{\mathbf{Cu}}_{\mathrm{isolated}} = [2.060, 2.082, 2.346]$. Calculation parameters for $T = 70$ K: $\boldsymbol{g}^{\mathbf{Cu}} = [2.054, 2.084, 2.320]$, $g^{\mathrm{R}} = 2.007$, $J = -200$ cm^{-1}; $\boldsymbol{g}^{\mathbf{Cu}}_{\mathrm{isolated}} = [2.060, 2.082, 2.346]$.

One can characterize spin transitions according to the abruptness of the transition (ΔT_{c}, typical temperature width), the characteristic mean temperature where it occurs (T_{c}), and its amplitude ($\Delta\mu_{\mathrm{eff}}$ in magnetic susceptibility or Δg_{eff} in EPR). In general, these three characteristics describe the spin transition essentially and allow for the qualitative conclusions on its cause and a magnitude of exchange interaction. For example, the high-temperature transition implies a larger magnitude of J compared to the low-temperature transition of the same abruptness and amplitude. This is obvious because smaller changes of J are required at low temperatures to vary parameter $|J|/kT$ to the same extent as at high temperatures (eqs 7 and 10). The abruptness of the spin transition characterizes the contribution of $J(T)$ dependence into the spin dynamics of a triad. A very abrupt transition implies the jumplike change of J, whereas a very gradual one implies slow changing with temperature or a nearly constant J. Finally, the amplitude of the spin transition is directly linked to the scale of the exchange interaction and its change, as is clear from eqs 7 and 10.

Cu(hfac)$_2$L$^{\mathrm{Bu}}$•0.5C$_7$H$_{16}$ (heptane) exhibits very abrupt spin transition at $T_{\mathrm{c}} \approx 125$ K, leading to a decrease in the effective

magnetic moment by $\Delta\mu_{eff} \approx 0.35\ \beta$ within a temperature range $\Delta T_c \approx 10$ K (Figure 4, inset). The overall decrease in the magnetic moment between $T = 300$ and 50 K is $\Delta\mu_{eff} \approx 2.53-1.85 = 0.68\ \beta$. The magnetic behavior below ~25 K is influenced by the intercluster exchange interaction between paramagnetic centers in the polymer chains, and we do not discuss it for this and other compounds in the present study. Figure 3 allows one to find a correlation between manifestations of spin transition in the magnetic susceptibility and in the EPR of $Cu(hfac)_2L^{Bu}\cdot 0.5C_7H_{16}$. The decrease of $\Delta\mu_{eff} \approx 0.7\ \beta$ down to $\mu_{eff} \approx 1.85\ \beta$ brings the spin triad from the situation $|J|/kT \ll 1$ to $|J|/kT > 1$ (part a of Figure 3). On the other hand, part b of Figure 3 shows that, for $|J|/kT > 1$ the values $g_{eff} < 2$ are expected, and thus intense EPR signals in the high-field region of the spectra should be observed. Of course, this use of part a of Figure 3 is only a helpful estimation, because the account of the exact g values as well as the weak exchange between one-spin and three-spin systems should influence the absolute values of the dependence $\mu_{eff}(|J|/kT)$ to some extent. In this respect, EPR data provides more direct information on the exchange interaction within a spin triad, because the exact g tensors are obtained and the contributions of one- and three-spin systems are well separated. The EPR spectra of $Cu(hfac)_2L^{Bu}\cdot 0.5C_7H_{16}$ exhibit drastic transformations near the transition temperature and show very intense signals in the $g < 2$ region for $T < 130$ K, which are well-resolved even at the X band (part a of Figure 4). As was explained by us in refs 24−25, this shape of the EPR spectra unambiguously indicates that the condition $|J|/kT > 1$ is fulfilled for the spin triad. There are almost no further transformations of the spectra between $T = 70$ and 110 K (part b of Figure 4), meaning that the spin transition is essentially completed below 110 K. This allows one to use the estimation $|J| > 2kT \approx 150$ cm^{-1} at $T < 110$ K. The X- and Q-band spectra at $T = 70$ and 110 K can be well simulated using the g tensors $\boldsymbol{g}^{Cu}$= [2.054, 2.084, 2.320] ($T = 70$ K) and $\boldsymbol{g}^{Cu}$=[2.048, 2.078, 2.314] ($T = 110$ K). The closeness of g tensors at two temperatures allows for the conclusion that, at $T < 70$ K, $\boldsymbol{g}_{eff} \approx \boldsymbol{g}^{A} \approx$ [1.993, 1.983, 1.905]. Apparently, the slight decrease of μ_{eff} at $T = 110-50$ K is primarily due to the antiferromagnetic intercluster interactions between spin triads and isolated copper spins. At temperatures above the spin transition at $T > 150$ K, the Q-band EPR spectra show the single broadened EPR line of a spin triad due to the electron spin exchange process. This line almost does not shift between 160 and 240 K, indicating that the limit $|J|/kT \ll 1$ is nearly achieved. The effective g factor of this EPR line at $T = 160$ K is $g_{eff} \approx 2.03$, in compliance with the situation $|J|/kT < 1$ (part b of Figure 3). Thus, we observe that the temperature-dependent EPR spectra of $Cu(hfac)_2L^{Bu}\cdot 0.5C_7H_{16}$ are indicative of the abrupt spin transition occurring in three-spin clusters >N−•O−Cu(II)−O•−N< by passing from the situation $|J|/kT < 1$ to a situation $|J|/kT > 1$. The temperature dependence of the EPR spectra is fully consistent with the magnetic susceptibility data above, below, and during the spin transition.

The magnetic susceptibility and EPR behavior of the compound $Cu(hfac)_2L^{Bu}\cdot 0.5C_8H_{16}$ (octene) are quite similar

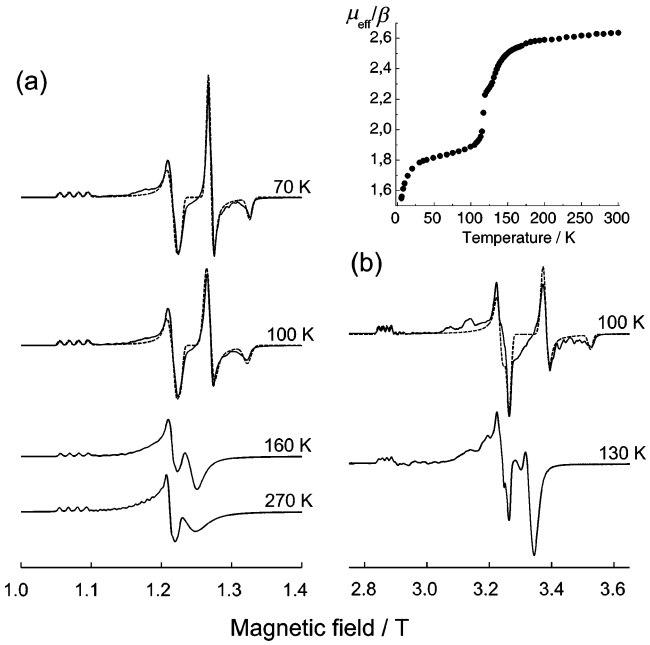

Figure 5. CW EPR spectra at different T (a,b) and dependence $\mu_{eff}(T)$ (inset) of $Cu(hfac)_2L^{Bu}\cdot 0.5C_8H_{16}$. (a) Q band ($\nu_{mw} \approx 35.343$ GHz, $B \approx 1.263$ T at $g_{eff} = 2$). (b) W band ($\nu_{mw} \approx 94.190$ GHz, $B \approx 3.365$ T at $g_{eff} = 2$). The temperatures are indicated on the right; the curves are scaled. Calculation parameters for $T = 100$ K: $\boldsymbol{g}^{Cu} = [2.040, 2.060, 2.300]$, $g^R = 2.007$, $J = -200$ cm^{-1}; $\boldsymbol{g}^{Cu}_{isolated} = [2.062, 2.081, 2.350]$. Calculation parameters for $T = 70$ K: $\boldsymbol{g}^{Cu} = [2.048, 2.068, 2.314]$, $g^R = 2.007$, $J = -200$ cm^{-1}; $\boldsymbol{g}^{Cu}_{isolated} = [2.062, 2.081, 2.350]$.

to the $Cu(hfac)_2L^{Bu}\cdot 0.5C_7H_{16}$ (Figure 5). The strong decrease of μ_{eff} is observed below $T \approx 150$ K, which is followed by an extremely abrupt ($\Delta T_c \approx 4$ K) jump down by ~$0.25\ \beta$ within $T \approx 119-115$ K. The overall decrease of the magnetic moment between $T = 200$ and 70 K is $\Delta\mu_{eff} \approx 2.59-1.83 = 0.76\ \beta$. The comparison of parts a and b of Figure 3 leads to a straightforward conclusion that the spin transition brings the system from the situation $|J|/kT < 1$ to $|J|/kT > 1$. Very intense and well-resolved $g < 2$ signals are observed at $T < 100$ K, and only a minor evolution of them occurs within $T = 100-70$ K (part a of Figure 5), allowing for an estimation $|J| > 2kT \approx 140$ cm^{-1} at $T < 100$ K. The Q- and W-band EPR spectra at $T = 100$ K can be well simulated using the g tensor $\boldsymbol{g}^{Cu} = [2.040, 2.060, 2.300]$, and the Q-band spectrum at $T = 70$ K using $\boldsymbol{g}^{Cu} = [2.048, 2.068, 2.314]$. The closeness of the g tensors at 70 and 100 K is an additional confirmation of the above estimate $|J| > 2kT$ and implies that, at $T < 70$ K, $\boldsymbol{g}_{eff} \approx \boldsymbol{g}^{A} \approx [1.993, 1.987, 1.905]$. The shape of the W-band spectrum of the isolated copper ion (one-spin unit) could not be simulated satisfactorily for this and several other compounds of the family, and the reason for this is currently unclear. However, our study is mainly focused on the EPR spectra of spin triads that are fairly described. Some decrease of μ_{eff} within $T = 100-40$ K is apparently due to the intercluster exchange between one-spin and three-spin systems. At temperatures above the transition $T > 150$ K, the single-spin exchange-narrowed EPR line of a triad is observed with the effective $g > 2.04$, meaning that the condition $|J|/kT < 1$ is fulfilled (part b of Figure 3). Thus, one concludes that the characteristics of the

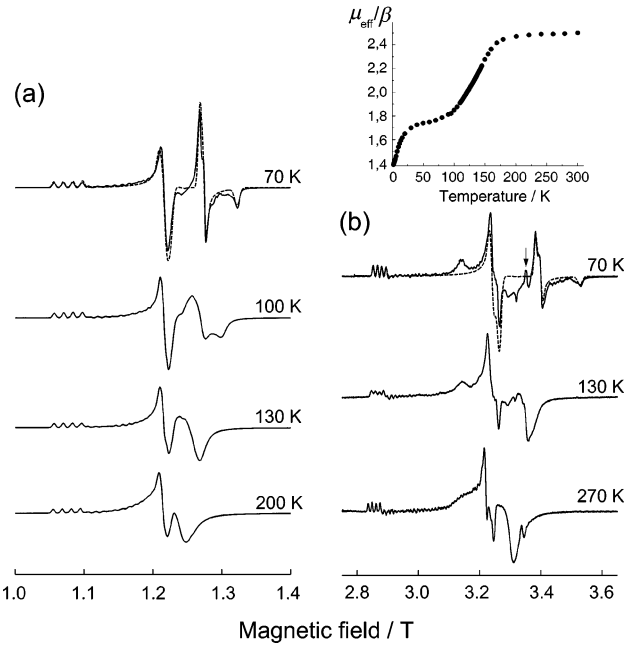

Figure 6. CW EPR spectra at different T (a,b) and dependence $\mu_{eff}(T)$ (inset) of $Cu(hfac)_2L^{Bu}\cdot 0.5C_8H_{18}$. (a) Q band ($\nu_{mw} \approx 35.320$ GHz, $B \approx 1.262$ T at $g_{eff} = 2$). (b) W band ($\nu_{mw} \approx 94.200$ GHz, $B \approx 3.365$ T at $g_{eff} = 2$). The temperatures are indicated on the right, the curves are scaled, and the arrow on the top trace (b) indicates the position of the signal from nitroxide defects. Calculation parameters for $T = 70$ K: $\boldsymbol{g}^{Cu} = [2.058, 2.090, 2.304]$, $g^R = 2.007$, $J = -115$ cm^{-1}; $\boldsymbol{g}^{Cu}_{isolated} = [2.062, 2.078, 2.343]$.

spin transition are similar for both $Cu(hfac)_2L^{Bu}\cdot 0.5C_8H_{16}$ and $Cu(hfac)_2L^{Bu}\cdot 0.5C_7H_{16}$.

$Cu(hfac)_2L^{Bu}\cdot 0.5C_8H_{18}$ (octane) represents an intermediate case between abrupt and gradual spin transitions (Figure 6). The dependence of the effective magnetic moment displays the nearly linear decrease by $\Delta\mu_{eff} \approx 0.6\,\beta$ within $T = 170-100$ K, and the overall decrease within $T = 240-60$ K is $\Delta\mu_{eff} \approx 0.74\,\beta$. The values $\mu_{eff} < 1.81\,\beta$ at $T < 90$ K unambiguously imply that the condition $|J| > kT$ is achieved. The transformations of the Q-band EPR spectra with temperature are fully consistent with this dependence. The gradual transformation of the single line into a line with a resolved g anisotropy is observed upon lowering the temperature to between 200 and 70 K, which is accompanied by a gradual shift of the line position toward lower g values (higher fields). The position of the EPR line of a spin triad at $T = 130$ K is close to 2, allowing for the estimation $|J| \approx kT \approx 90$ cm^{-1}. The Q- and W-band EPR spectra at 70 K can be simulated using $\boldsymbol{g}^{Cu} = [2.058, 2.090, 2.304]$, and thus $\boldsymbol{g}_{eff} \approx \boldsymbol{g}^{A} \approx [1.990, 1.979, 1.908]$. Because the major transformation has already occurred at $T = 70$ K, one can estimate $|J| > 2kT \approx 100$ cm^{-1} at $T < 70$ K.

The studies of the compound $Cu(hfac)_2L^{Pr}$ have already been reported by us in refs 24−25. The temperature dependence of the effective magnetic moment shows a gradual decrease from $\mu_{eff} \approx 2.55\,\beta$ at $T = 260$ down to $\mu_{eff} \approx 1.82\,\beta$ at 60 K (Figure 7, inset). A structural phase transition occurs at $T = 226$ K;[15,16] however, it has only a minor effect on the curve $\mu_{eff}(T)$ ($\Delta\mu_{eff}$ is small near 226 K). The EPR spectra exhibit gradual transformations upon lowering the temperature similar to that for the previous

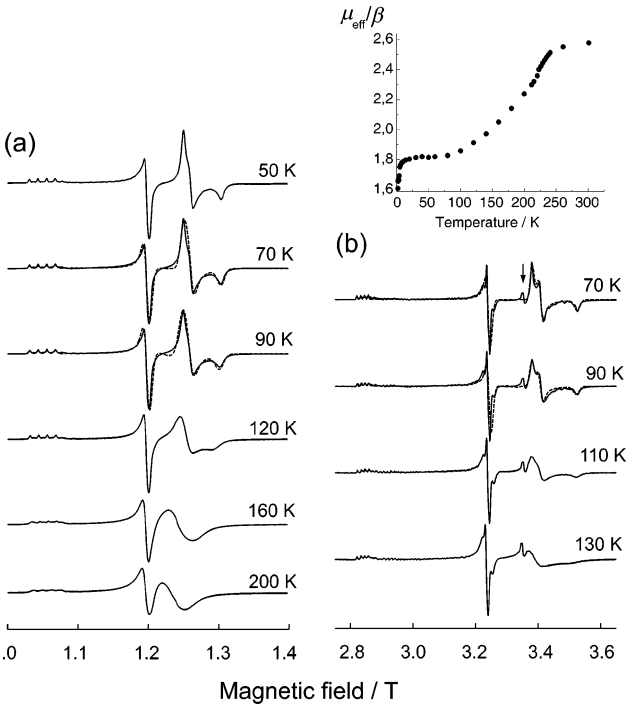

Figure 7. CW EPR spectra at different T (a,b) and dependence $\mu_{eff}(T)$ (inset) of $Cu(hfac)_2L^{Pr}$. (a) Q band ($\nu_{mw} \approx 34.832$ GHz, $B \approx 1.244$ T at $g_{eff} = 2$). (b) W band ($\nu_{mw} \approx 94.245$ GHz, $B \approx 3.367$ T at $g_{eff} = 2$). The temperatures are indicated on the right, the curves are scaled, and the arrow on the top trace (b) indicates the position of the signal from nitroxide defects. Calculation parameters for $T = 90$ K: $\boldsymbol{g}^{Cu} = [2.047, 2.097, 2.290]$, $g^R = 2.007$, $J = -115$ cm^{-1}; $\boldsymbol{g}^{Cu}_{isolated} = [2.075, 2.075, 2.371]$. Calculation parameters for $T = 70$ K: $\boldsymbol{g}^{Cu} = [2.055, 2.105, 2.300]$, $g^R = 2.007$, $J = -135$ cm^{-1}; $\boldsymbol{g}^{Cu}_{isolated} = [2.075, 2.075, 2.371]$.

compound $Cu(hfac)_2L^{Bu}\cdot 0.5C_8H_{18}$ but on a broader temperature range (Figure 7). The position of the EPR line of spin triad corresponds to $g_{eff} \approx 2$ at quite high temperature $T \approx 170$ K, which implies a strong exchange interaction $|J| \approx kT \approx 115$ cm^{-1}. At $T < 90$ K, the transformations of the spectra are mostly completed, which allows for the estimation $|J| > 2kT \approx 125$ cm^{-1}. This relatively slow increase of the exchange interaction between 170 and 90 K is consistent with the gradual decrease of μ_{eff} and with structural changes obtained in X-ray studies (Figure 2).[15,16] Note that these estimations of J are close to the value $J = -100$ cm^{-1} obtained in ref 15 using a simplified analysis in a model of the constant exchange interaction. Comparing the gradual spin transition in $Cu(hfac)_2L^{Pr}$ with abrupt spin transitions in our first two examples, it is evident that the $J(T)$ function in $Cu(hfac)_2L^{Pr}$ is much more flat, and thus the spin transition is stronger, contributed by a simple decrease in temperature in parameter $|J|/kT$. At low temperatures, the Q- and W-band spectra can be simulated using $\boldsymbol{g}^{Cu} = [2.047, 2.097, 2.290]$ ($T = 90$ K) and slightly different $\boldsymbol{g}^{Cu} = [2.055, 2.105, 2.300]$ ($T = 70$ K), thus one finds $\boldsymbol{g}_{eff} \approx \boldsymbol{g}^{A} \approx [1.991, 1.974, 1.909]$ at $T < 70$ K.

The dependence $\mu_{eff}(T)$ of the compound $Cu(hfac)_2L^{Bu}\cdot 0.5C_8H_{10}$ (*o*-xylene) is very similar to the one of $Cu(hfac)_2L^{Pr}$ (Figure 8). An even more-gradual spin transition in the wider temperature range $T = 300-50$ K is observed with the overall decrease $\Delta\mu_{eff} \approx 0.68\,\beta$ down to the value $\mu_{eff}(50K) \approx 1.8\,\beta$, which assumes $|J| > kT$. The changes of EPR

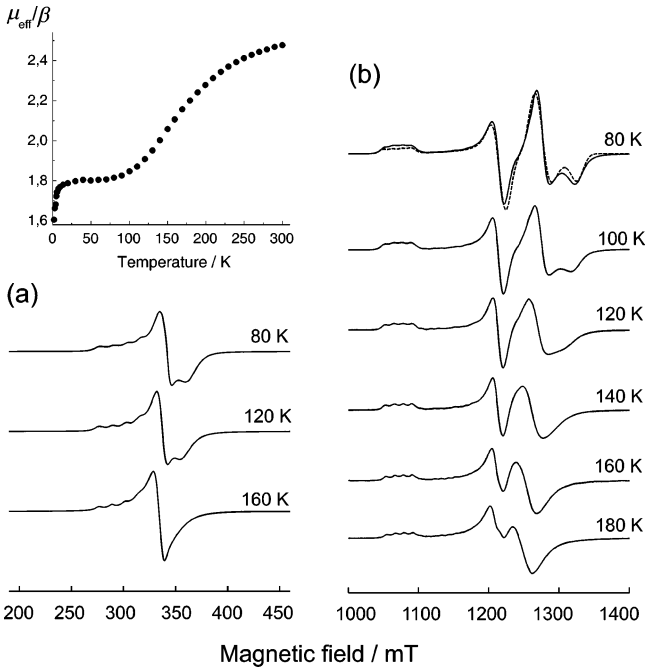

Figure 8. CW EPR spectra at different T (a,b) and dependence $\mu_{eff}(T)$ (inset) of Cu(hfac)$_2$L^{Bu}·0.5C$_8$H$_{10}$. (a) X band ($\nu_{mw} \approx 9.710$ GHz, $B \approx 347$ mT at $g_{eff} = 2$). (b) Q band ($\nu_{mw} \approx 35.335$ GHz, $B \approx 1262$ mT at $g_{eff} = 2$). The temperatures are indicated on the right; the curves are scaled. Calculation parameters for the Q-band spectrum at $T = 80$ K: $\boldsymbol{g}^{Cu} = [2.063, 2.078, 2.314]$, $g^R = 2.007$, $J = -100$ cm^{-1}; $\boldsymbol{g}^{Cu}_{isolated} = [2.060, 2.082, 2.360]$.

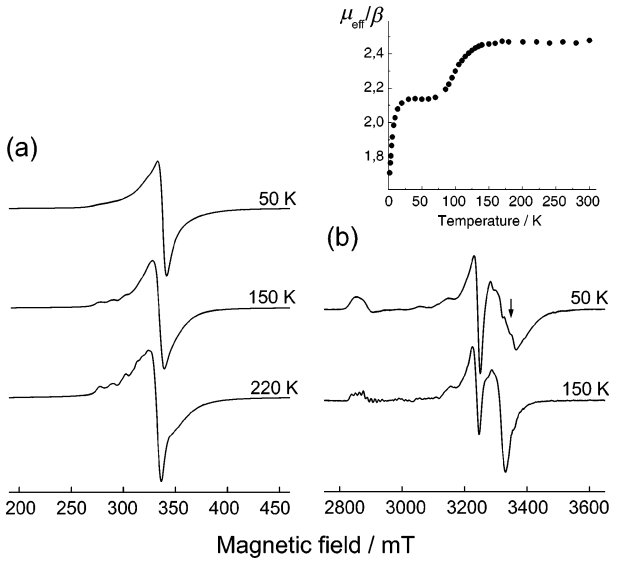

Figure 9. CW EPR spectra at different T (a,b) and dependence $\mu_{eff}(T)$ (inset) of Cu(hfac)$_2$L^{Bu}·0.5C$_7$H$_8$. (a) X band ($\nu_{mw} \approx 9.70$ GHz, $B \approx 347$ mT at $g_{eff} = 2$). (b) W band ($\nu_{mw} \approx 94.250$ GHz, $B \approx 3367$ mT at $g_{eff} = 2$). The temperatures are indicated on the right; the curves are scaled, and the arrow on the top trace (b) indicates the position of the signal from nitroxide defects.

spectra are easily observed even at the X-band; however, the $g < 2$ signals are very broad, which complicates the interpretation. These broad lines are apparently due to the slower rate of electron spin exchange, as was already proposed by us for this compound in ref 25. The Q-band spectra are already well resolved and allow one to trace the gradual temperature evolution of EPR spectra, as was done for Cu(hfac)$_2$L^{Pr} above. At $T < 100$ K, the position of the EPR line of a spin triad is almost temperature-independent, thus $|J| > 2kT \approx 140$ cm^{-1}. The spectrum at $T = 80$ K can be simulated using $\boldsymbol{g}^{Cu} = [2.063, 2.078, 2.314]$ ($\boldsymbol{g}_{eff} \approx \boldsymbol{g}^{A} \approx [1.998, 1.983, 1.905]$). Resuming, the temperature evolution of EPR spectra is fully consistent with the magnetic susceptibility data for gradual spin transitions, as well as it was shown above for the abrupt ones.

So far, we have discussed those compounds of family Cu(hfac)$_2$L^R, which exhibit pronounced spin transitions bringing a spin triad into the condition $|J| > kT$. Now, we are going to discuss those compounds that exhibit only minor changes of the effective magnetic moment during the spin transitions. In all of these cases, we did not succeed to detect the resolved signals with $g < 2$ at available temperatures, but still, all of the observed trends were in complete agreement with the above phenomenological model, and useful information on spin triads was obtained.

Cu(hfac)$_2$L^{Bu}·0.5C$_7$H$_8$ (toluene) is a good example of an intermediate case between compounds exhibiting pronounced and minor spin transitions (Figure 9). The dependence $\mu_{eff}(T)$ displays a rather gradual transition occurring at temperature range ~150−70 K with the amplitude $\Delta\mu_{eff} \approx 0.32\ \beta$. In many respects, this shape of the curve $\mu_{eff}(T)$ is similar to the one of Cu(hfac)$_2$L^{Bu}·0.5C$_8$H$_{18}$; however, its amplitude is smaller by a factor of about 2. The value μ_{eff} (70 K) $\approx 2.15\ \beta$ implies that at this temperature $|J|/kT \approx 0.6$, and thus $g_{eff} \approx 2.03 > 2$ is expected (Figure 3). Indeed, these expectations describe the experimental EPR spectra very well (Figure 9). The X-band data do not allow one to observe considerable changes in EPR spectra during the spin transition. It was also not possible to observe a significant shift of a line of a spin triad at the W band. However, W-band spectra clearly show the change of the line shape of a spin triad at the $g \approx 2$ region (part b of Figure 9), which can be interpreted by a slight shift of a still broad EPR line of a spin triad toward the higher fields (smaller g values). Thus, we conclude that the decrease of the g_{eff} of a spin triad does occur during the spin transition; however, its amplitude Δg_{eff} is too small to be safely detected at the W band, which supposes the small magnitude of the exchange interaction and its change. We can roughly estimate the value of exchange interaction at $T < 50$ K from the condition $|J| < kT \approx 35$ cm^{-1}.

Even smaller changes of g_{eff} during the spin transition are observed for the compounds Cu(hfac)$_2$L^{Bu}·0.5C$_6$H$_6$ (benzene) ($T_c \approx 47$ K, $\Delta T_c \approx 30$ K, $\Delta\mu_{eff} \approx 0.15\ \beta$) and Cu(hfac)$_2$L^{Bu}·0.5C$_6H_{14}$ (hexane) ($T_c \approx 160$ K, $\Delta T_c \approx 25$ K, $\Delta\mu_{eff} \approx 0.17\ \beta$). In both cases, the EPR signals of the isolated copper ion and spin triad are resolved already at the Q band (Figures 10 and 11); however, the shift of the EPR line of a triad is very small during a spin transition. This is expected indeed for such small values of $\Delta\mu_{eff}$ as ~0.15−0.17 β, when μ_{eff} is not smaller than ≈2.2 β after a transition. Using Figure 3, one estimates that $|J|/kT \approx 0.25$ at $\mu_{eff} \approx 2.2\ \beta$, leading to $\Delta g_{eff} \approx 0.005$ only.

The compound Cu(hfac)$_2$L^{Bu} without a solvent is another example of a small-amplitude spin transition ($T_c \approx 75$ K, $\Delta T_c \approx 15$ K, $\Delta\mu_{eff} \approx 0.16\ \beta$), which also does not lead to

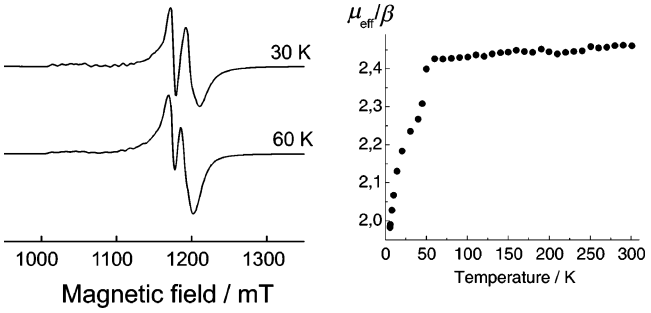

Figure 10. Q-band CW EPR spectra at different T and dependence μ_{eff}-(T) (inset) of Cu(hfac)$_2$L^{Bu}·0.5C$_6$H$_6$ ($\nu_{mw} \approx 34.183$ GHz, $B \approx 1221$ mT at $g_{eff} = 2$). The temperatures are indicated on the right; the curves are scaled.

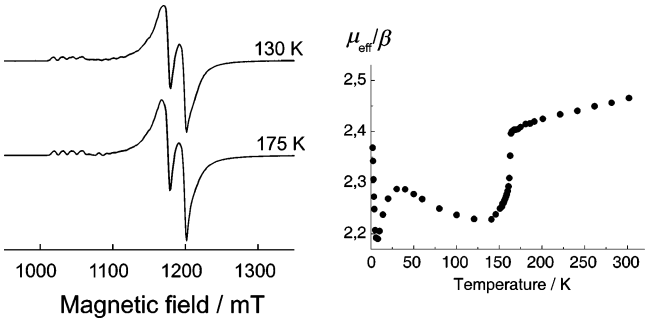

Figure 11. Q-band CW EPR spectra at different T and dependence μ_{eff}-(T) (inset) of Cu(hfac)$_2$L^{Bu}·0.5C$_6$H$_{14}$ ($\nu_{mw} \approx 34.181$ GHz, $B \approx 1.221$ T at $g_{eff} = 2$). The temperatures are indicated on the right; the curves are scaled.

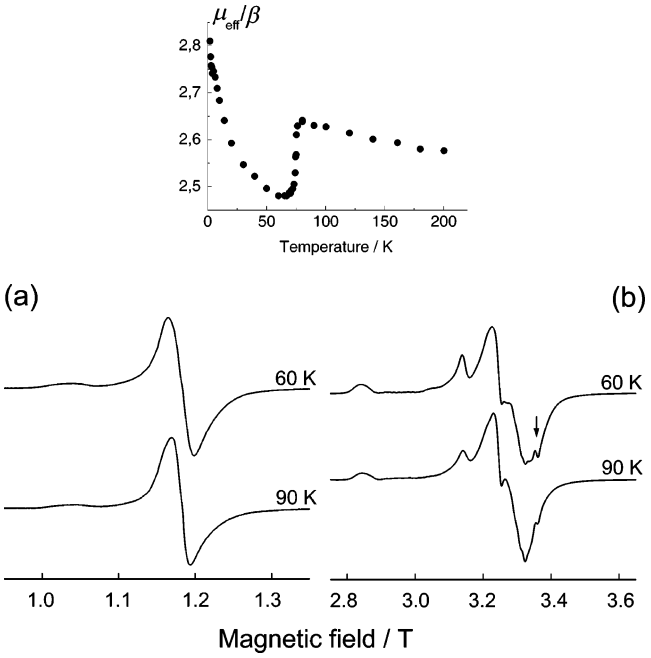

Figure 12. CW EPR spectra at different T (a,b) and dependence $\mu_{eff}(T)$ (inset) of Cu(hfac)$_2$L^{Bu}. (a) Q band ($\nu_{mw} \approx 34.181$ GHz, $B \approx 1.221$ T at $g_{eff} = 2$). (b) W band ($\nu_{mw} \approx 94.304$ GHz, $B \approx 3.369$ T at $g_{eff} = 2$). The temperatures are indicated on the right, the curves are scaled, and the arrow on the top trace (b) indicates the position of the signal from nitroxide defects.

significant changes in the EPR spectra (Figure 12). It is interesting that the slope of the magnetic susceptibility dependence corresponds to a weak ferromagnetic exchange coupling, but at the same time μ_{eff} abruptly decreases during the spin transition. The possible explanation of this behavior is the presence of a weak intercluster ferromagnetic exchange between one- and three-spin systems, whereas the exchange

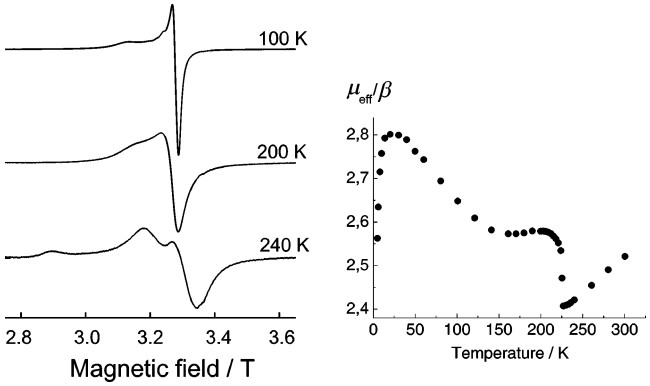

Figure 13. W-band CW EPR spectra at different T and dependence μ_{eff}-(T) (inset) of Cu(hfac)$_2$L^{Et} ($\nu_{mw} \approx 94.300$ GHz, $B \approx 3.369$ T at $g_{eff} = 2$). The temperatures are indicated on the right; the curves are scaled.

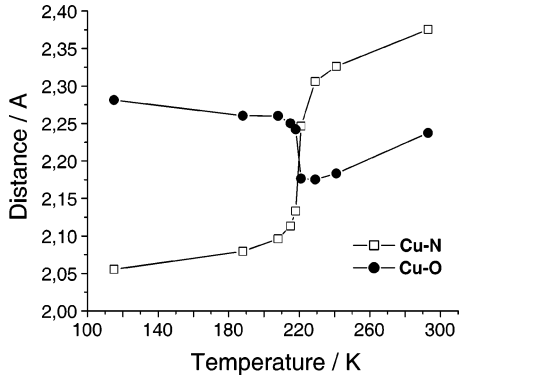

Figure 14. Temperature dependences of the Cu−O$_L$ (CuO$_6$ unit) and Cu−N$_L$ (CuO$_4$N$_2$ unit) distances in Cu(hfac)$_2$L^{Et} obtained by X-ray study (O$_L$ and N$_L$ atoms belong to the nitroxide groups).

interaction within a spin-triad J is antiferromagnetic, and thus the spin transition occurs following the same scenario as discussed above. In contrast to the cases of Cu(hfac)$_2$L^{Bu}·0.5C$_6$H$_6$ and Cu(hfac)$_2$L^{Bu}·0.5C$_6$H$_{14}$, the EPR signals of the isolated copper ion and the spin triads in Cu(hfac)$_2$L^{Bu} are poorly resolved even at the W band (part b of Figure 12), which might be due to a stronger intercluster exchange interaction compared to that of the two former cases. A slight shift of the EPR line of a triad toward smaller g values is observed between 90 and 60 K, which is indicative of a weak antiferromagnetic exchange interaction J within a triad. Thus, the EPR data fully supports the above hypothesis and is also in agreement with the theoretical expectations.

The last example presented in this work Cu(hfac)$_2$L^{Et} ($T_c \approx 226$ K, $\Delta T_c \approx 5$ K, $\Delta\mu_{eff} \approx 0.15\ \beta$) shows the completely different dependence $\mu_{eff}(T)$, compared to all of the cases described above (Figure 13). Upon lowering the temperature in the range ~300−226 K, the magnetic moment decreases, manifesting a strong antiferromagnetic coupling within a spin triad; however, the spin transition leads to an increase of μ_{eff}. This can be explained by an abrupt decrease of the antiferromagnetic coupling or even a change of its sign during the spin transition, which is consistent with the abrupt lengthening of the Cu−O distances below 226 K (Figure 14).[15,16] In any case, this kind of transition should lead to an opposite shift of g_{eff}, that is, to its increase, as opposed to all of the situations discussed above. The comparison of W-band EPR spectra at 240 and 200 K shows that exactly

Table 1. The Characteristic Changes of the Effective Magnetic Moment ($\Delta\mu_{eff}$) and Effective g Factor of a Triad (Δg_{eff}) During Spin Transitions. The estimations of the absolute value of the exchange interaction ($|J|$) within a spin triad ($J<0$, i.e., the exchange interaction is antiferromagnetic)[a]

					$\mathbf{g}_{eff}$	$\mathbf{g}^{Cu}$
compound	$\Delta\mu_{eff}$	Δg_{eff}	$\lvert J\rvert$ (cm^{-1}) at T (K)		for $\lvert J\rvert/kT \gg 1$	
$Cu(hfac)_2L^{Bu}\cdot 0.5C_7H_{16}$	~0.68	~0.072	>150	$T < 110$	[1.993, 1.983, 1.905]	[2.048, 2.078, 2.314]
$Cu(hfac)_2L^{Bu}\cdot 0.5C_8H_{16}$	~0.76	~0.078	>140	$T < 100$	[1.993, 1.987, 1.905]	[2.048, 2.068, 2.314]
$Cu(hfac)_2L^{Bu}\cdot 0.5C_8H_{18}$	~0.74	~0.087	>100	$T < 70$	[1.990, 1.979, 1.908]	[2.058, 2.090, 2.304]
$Cu(hfac)_2L^{Pr}$	~0.73	~0.072	>125	$T < 90$	[1.991, 1.974, 1.909]	[2.055, 2.105, 2.300]
$Cu(hfac)_2L^{Bu}\cdot 0.5C_8H_{10}$	~0.68	~0.078	>140	$T < 100$	[1.998, 1.983, 1.905]	[2.063, 2.078, 2.314]
$Cu(hfac)_2L^{Bu}\cdot 0.5C_7H_8$	~0.32	~0.010	<35	$T < 50$		
$Cu(hfac)_2L^{Bu}\cdot 0.5C_6H_6$	~0.15	~0.014	<20	$T < 30$		
$Cu(hfac)_2L^{Bu}\cdot 0.5C_6H_{14}$	~0.17	<0.002	≪90	$T < 130$		
$Cu(hfac)_2L^{Bu}$	~0.16	<0.006	<40	$T < 60$		
$Cu(hfac)_2L^{Et}$	~0.15	~0.021	≪140	$T < 200$		

[a] The effective g tensors of a triad ($\boldsymbol{g}_{eff}$) and the copper ion included in a triad ($\boldsymbol{g}^{Cu}$) are used in simulations for the case $|J|/kT \gg 1$ with a typical accuracy of less than ±0.003.

this is observed in experiment. The EPR lines of the isolated copper ion and the spin triad are not resolved, but the disappearance of the broad high-field wing of this overlapped line at 200 K is obvious. Thus, the EPR study of $Cu(hfac)_2L^{Et}$ nicely illustrates that the approaches developed work for reverse transitions (when $|J|/kT$ decreases) as well.

Finally, Table 1 summarizes the results of the presented study on the family of compounds $Cu(hfac)_2L^R$. One observes a good correlation between $\Delta\mu_{eff}$ and Δg_{eff}. For the compounds with a strong exchange interaction within a spin triad, the useful estimates of its value are obtained. For those with a weaker exchange coupling, the estimates are less accurate and useful. But, in all of the cases the EPR behavior agrees completely with the magnetic susceptibility data, and the use of simple rules for the positions of the EPR signals allows for estimations of J and characterization of spin transitions.

IV. Conclusions

Using numerous examples we have demonstrated the efficiency of EPR for the study of thermally induced spin transitions and exchange interactions in spin triads of nitroxide−copper(II)−nitroxide. Our previous results on the general characteristics of strongly coupled spin triads[24,25] have been successfully applied in this work for the EPR study and classification of magnetic anomalies in the family $Cu(hfac)_2L^R$. The manifestations of spin transitions in both magnetic susceptibility and EPR data can be understood using a simple phenomenological model, where the dependencies of the effective magnetic moment μ_{eff} and the effective g factor of a spin triad g_{eff} are considered as functions of the parameter $|J(T)|/kT$. If $|J|/kT \ll 1$, all of the total spin states of a triad (two doublets and one quartet) are almost equally populated, but if $|J|/kT \gg 1$ the ground state becomes predominately populated. Thus, the passage between situations $|J|/kT \ll 1$ and $|J|/kT \gg 1$ leads to the changes in the effective magnetic moment value and in the EPR spectra. In most of the cases, the strong dependence $J(T)$ occurring due to the structural rearrangements is the driving force of these spin transitions. Very informative EPR spectra are observed if the transition leads to a strong increase in $|J|$ and brings the spin system into condition $|J| > kT$. In this case, it is straightforward to determine the sign of J and to estimate its magnitude $|J|$ by monitoring the temperature-dependent position of the EPR line of a triad. In particular, intense signals with typical g values of $g < 2$ are indicative of the strong antiferromagnetic exchange interaction $|J| > kT$. The absence of these signals, instead, is indicative of the ferromagnetic or weak antiferromagnetic coupling ($|J| < kT$). Different kinds of spin transitions occurring at a wide range of temperatures $T \approx 50-230$ K are studied using X-, Q-, and W-band CW EPR spectroscopy. All of the obtained results agree well with the phenomenological model, as well as with the previous magnetic susceptibility and X-ray data.

We have thus demonstrated that EPR can be employed as a useful alternative to the magnetic susceptibility technique for the studies of strongly coupled spin triads, especially when the exchange interaction in a triad is antiferromagnetic. In this case, EPR provides for more accurate information on the dependence $J(T)$ due to the direct determination of g tensors and due to the possibility of the selective study of the exchange interaction within a spin triad. The EPR approaches described by us in this work can be used in future studies of spin transitions and exchange interactions in various strongly coupled heterospin clusters.

Acknowledgment. We gratefully acknowledge the participation of Prof. Arthur Schweiger (ETH Zürich) in the early stages of this project. We thank Prof. V. N. Ikorskii for the magnetic susceptibility measurements. This work was supported by INTAS (Grants YSF 04-83-2669 and YSF 06-1000014-5915), RFBR (Grants 05-03-32264, 06-03-32157, and 06-03-04000), Lavrentiev grant of SB RAS (Grant 79), RF president (Grants MK-6673.2006.3 and MK-10264.2006.3), FASI state contract number 02.513.11.3044, RAS, and the Swiss National Foundation.

Supporting Information Available: Crystallographic data in CIF format. This material is available free of charge via the Internet at http://pubs.acs.org.

IC7014385